

Measurement of relative electron-impact-excitation cross sections for Fe^{24+}

C. M. Brown, U. Feldman, G. A. Doschek, J. F. Seely, and R. E. LaVilla

E. O. Hulburt Center for Space Research, Naval Research Laboratory, Washington, D.C. 20375-5000

V. L. Jacobs

Condensed Matter and Radiation Sciences Division, Naval Research Laboratory, Washington, D.C. 20375-5000

J. R. Henderson, D. A. Knapp, R. E. Marrs, and P. Beiersdorfer

University of California, Lawrence Livermore National Laboratory, Livermore, California 94550

M. A. Levine

University of California, Lawrence Berkeley Laboratory, Berkeley, California 94720

(Received 17 April 1989)

We present measurements of the relative electron-impact-excitation cross sections for the $1s^2\ ^1S_0-1s2p\ ^1P_1$, $1s^2\ ^1S_0-1s2p\ ^3P_2$, $1s^2\ ^1S_0-1s2p\ ^3P_1$, and $1s^2\ ^1S_0-1s2s\ ^3S_1$ transitions for the He-like ion, Fe^{24+} . The measurements were made at two electron energies: 6.86 and 9.94 keV. The cross-section measurements are compared with theoretical calculations.

In this paper we present measurements of the electron-impact-excitation (IE) cross sections near the threshold energy E and at about $1.5E$ for the resonance ($1s^2\ ^1S_0-1s2p\ ^1P_1$), magnetic quadrupole ($1s^2\ ^1S_0-1s2p\ ^3P_2$), intercombination ($1s^2\ ^1S_0-1s2p\ ^3P_1$), and forbidden ($1s^2\ ^1S_0-1s2s\ ^3S_1$) lines of the He-like ion Fe^{24+} . The lines are referred to as w , x , y , and z , respectively.¹ These lines, as well as the same transitions in other solar-abundant He-like ions, have been observed in the spectra of solar flares.^{2,3} In addition, these transitions have been observed in tokamak spectra⁴⁻⁷ of He-like titanium, chromium, iron, and nickel.

The motivation for measuring cross sections for w , x , y , and z is that the solar and tokamak observations reveal apparent discrepancies between the measured line ratios, x/w , y/w , z/w , and theoretical calculations. The differences between theory and observation are complicated and variable, depending on the plasma conditions and temperature. The discrepancy for the solar iron spectra is noted by Lemen *et al.*⁸ and Doschek and Tanaka.² In particular, for the solar data the intensity ratio y/w is larger than calculated. The x/w and z/w ratios could also be larger than calculated, but for all line ratios the differences between theory and experiment depend on the abundance ratio of Fe^{25+} to Fe^{24+} in the flare plasma, which is uncertain. The tokamak discrepancies are discussed in some of the above referenced papers.

Theoretical calculations for the He-like ion lines are given in a number of papers.^{5,9-15} These calculations consider contributions due to direct excitation, excitation followed by cascade (IEC), radiative recombination (RR), and resonances. It is important to attempt to clarify the reasons for the discrepancies between observation and theory since the discrepancies might be caused by physical effects in the plasmas. For example, transient ionization in a plasma could produce an enhancement of line z due to innershell ionization of Fe^{23+} , and a non-

Maxwellian velocity distribution could alter the line ratios. Accurate cross sections are necessary to evaluate the effects of nonequilibrium plasma processes on line ratios.

The Fe^{24+} measurements were obtained using the electron beam ion trap (EBIT) at the Lawrence Livermore National Laboratory (LLNL). The EBIT and the measurement technique are described in detail elsewhere.^{16,17} Briefly, ions are injected, trapped in an approximately 2-cm-long electrostatic well, and ionized to a high charge state by an electron beam. The degree of ionization is adjusted by varying the energy of the electron beam. The electron beam is also used to excite the ions. Measurements are made by observing the x rays emitted upon the decay of excited states and upon radiative recombination. The energy of the electron-ion collisions is nearly monoenergetic with a width of approximately 50 eV full width at half maximum, making it possible to measure cross sections at discrete energies and to investigate separately different excitation processes in a particular ion.

The electron density in the beam is approximately $2 \times 10^{12}\ \text{cm}^{-3}$. For He-like ions with atomic number $Z \gtrsim 12$, populations of metastable levels are negligible compared to the ground level population, and therefore line ratios are not sensitive to electron density.

Different excitation processes in a particular ion can be investigated individually by varying the energy of the beam. In particular, the beam energy can be set at an energy slightly exceeding the IE threshold of a particular level, and the threshold IE cross section can be measured. At higher energies it is necessary to consider several additional atomic processes in order to interpret results.

Finally, it should be noted that in the experiments to be described below, radiation was detected in a direction perpendicular to the electron-beam direction with a curved crystal spectrometer. It is necessary to consider the anisotropy of the emission and polarization of the ra-

diation in interpreting the results.

Spectra of Fe^{24+} were obtained with a high-resolution curved-crystal spectrometer constructed jointly by the Naval Research Laboratory and the National Institute of Standards and Technology (NIST). The spectrometer is based on a Johann configuration employing a bendable crystal and a fixed detector-to-crystal distance. In an instrument of this type, changing the Bragg angle results in a change in the radius of the Rowland circle which requires a change in the radius of the crystal bend. This is accomplished with the crystal-bending apparatus, which is described by Henins.¹⁸ The crystal used was Ge(220) with a $2d$ spacing of 4.00 Å. The nominal Bragg angle was 27.55°. A Ho $L\alpha$ calibration source was used to help determine wavelengths and the spectrometer dispersion.

The detector is a position-sensitive sealed gas proportional counter manufactured by Deslattes and colleagues at NIST. A similar detector is described by Duval *et al.*¹⁹ The detector has a single anode wire and a double-wedge type cathode. The spatial resolution is about 200 μm . The detector gas is Xe with 10% CH_4 , at one atmosphere pressure. A 76- μm -thick Be window covered the detector aperture. The noise in the detector and associated electronics was only about 1–3 counts/channel away from spectral lines in integration times of several thousand seconds.

The EBIT source, approximately 2 cm long and 70 μm in diameter, was inside the Rowland circle, and the Ho calibration source was outside the Rowland circle. The electron beam was normal to the plane of dispersion of the spectrometer. Because of the small size of the EBIT source and the distance between the EBIT source and the crystal, only a small wavelength range could be viewed at the 27.55° Bragg angle. This range was about 14 mÅ, hence it was only possible to observe three of the four He-like lines simultaneously. The Bragg angle could be conveniently changed to alter the wavelengths incident on the detector.

The detector wedge pattern was perpendicular to the line of sight, and only one point on the detector was perfectly in focus on the Rowland circle. Therefore spectral resolution was not uniform over the detected wavelength range. However, the resolution was always sufficient to resolve fully the He-like iron spectrum. The sensitivity of the detector as a function of position (channel) on the cathode was measured with a radioactive source and found to be uniform within $\pm 3\%$.

In addition to the high-resolution curved-crystal spectrometer, a lower-resolution 5-mm-thick \times 6-mm-diam solid-state Ge detector provided by LLNL was used to observe the entire iron spectrum over a broad wavelength range. In particular, RR lines formed by capture into $n = 2, 3$ levels of Fe^{24+} were observed along with a broad IE feature composed of $w, x, y,$ and z , and an innershell excitation line from Fe^{23+} called q^1 . Line q is due to the transition, $1s^2 2s^2 S_{1/2} - 1s 2p(^1P) 2s^2 P_{3/2}$.

A term diagram of Fe^{24+} is shown in Fig. 1. The wavelengths in the figure are from solar observations by Seely *et al.*²⁰ We obtained spectra at electron-beam energies of 6.86 ± 0.01 , and at 9.94 ± 0.01 keV. These energies were determined to this precision from the centroids of

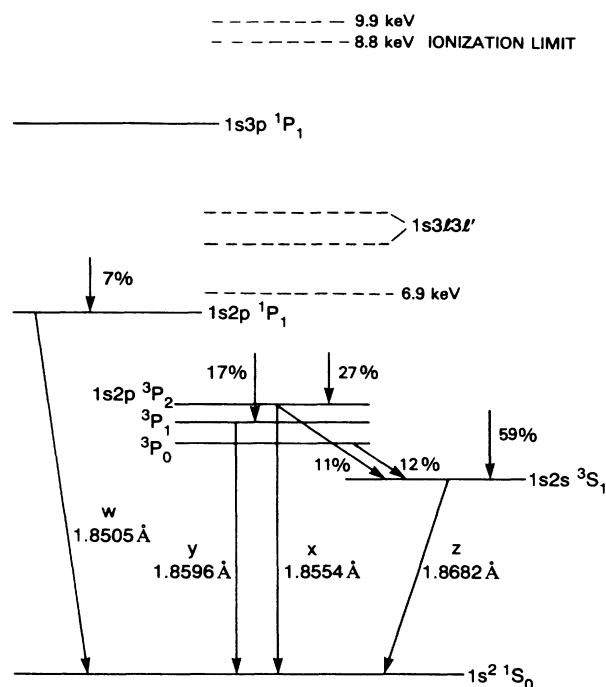


FIG. 1. Term diagram for He-like ions. The percentage figures give the fraction of the line intensity arising from excitation followed by cascade into the upper level of the line, for the 9.94-keV case. For example, 59% of the intensity of line z at 9.94 keV arises from excitation of levels with $n > 2$ followed by cascade into the $1s2s^3S_1$ level.

radiative recombination lines.

The interpretation of the 6.86-keV spectra is relatively straightforward. Because 6.86 keV is below bound-state excitation energies for $n \geq 3$, and because this energy is not coincident with a possible resonance due to dielectronic capture followed by autoionization into one of the excited states of $w, x, y,$ or z , there are no possible contributions from this process and IEC. Furthermore, there was very little Fe^{23+} in the trap, as evidenced by the small intensity of line q , which appears as an unresolved shoulder on the long-wavelength side of line y . At 6.86 and 9.94 keV the intensity of q was determined by modeling each line in the high-resolution spectra as a Gaussian peak of unknown amplitude and width, but constrained to a known wavelength. Only spectra where the y, q feature was fully within the observable wavelength win-

TABLE I. Fe^{24+} line ratios measured at 90° to the electron-beam axis and with the beam normal to the plane of spectral dispersion.

Electron-beam energy (keV)	x/w	y/w	z/w
6.86	0.18 ± 0.03	0.25 ± 0.04	0.24 ± 0.06
9.94	0.12 ± 0.02	0.20 ± 0.03	0.33 ± 0.06

dow were used. A nonlinear least-squares-fitting routine was used to determine the amplitude of each line. The reduced χ^2 value from fitting the data by this procedure was in the range of 0.85 to 1.17, indicating good agreement between the fitting model and the data. The observed intensity of q was $12 \pm 4\%$ the intensity of y .

The interpretation of the 9.94-keV spectra is more complicated because in this case the beam energy exceeds the ionization energy of Fe^{24+} . Inspection of the solid-state Ge detector spectra shows RR lines onto bare iron nuclei as well as onto H-like iron. Excitation of $n \geq 3$ levels of Fe^{24+} followed by cascade into $n = 2$ levels (IEC) is important, and radiative recombination contributions to the lines must also be considered. From analysis of the solid-state Ge detector spectra, we find the following percentages of iron ions: Fe^{23+} , $4 \pm 4\%$; Fe^{24+} , $56 \pm 5\%$; Fe^{25+} , $36 \pm 2\%$, and Fe^{26+} , $4 \pm 1\%$.

It was necessary to take two spectra in order to include all four Fe^{24+} lines. The 6.86-keV spectra are shown in Fig. 2. The 9.94-keV spectra appear similar to the lower-energy spectra. Spectra were integrated in time until a 1σ statistical uncertainty in the total intensity of the weakest line (usually x) was 10%.

The experimental ratios x/w , y/w , and z/w are given in Table I for both the 6.86- and 9.94-keV cases. We emphasize that these ratios refer to cross sections obtained at 90° to the electron beam, uncorrected for polarization effects. Lines w and y are $E1$ transitions, while line z is an $M1$ transition and line x is an $M2$ transition.

For the 6.86-keV case it is possible to take full account of the effects of polarization since these have been calculated by Inal and Dubau.¹⁵ The crystal we use is a perfect crystal (Henins²¹), and the reflectivities for parallel and perpendicular polarization have been calculated by Gullikson²² as a function of wavelength. The reflectivity of the perpendicular component is approximately propor-

tional to $\cos(2\theta)$, where θ is the Bragg angle.

Theoretical calculations of line ratios for the 6.86-keV case obtained from direct IE rates,^{10,13,15} including the effects of polarization, are given in Table II. The calculations take into account the fact that the $1s2p\ ^3P_0$ level decays only to the $1s2s\ ^3S_1$ level and that the branching ratio of $1s2p\ ^3P_2$ to $1s2s\ ^3S_1$ is 0.18. These are the expected theoretical line ratios obtained after diffraction by the crystal. Also given in parentheses are the line ratios obtained from calculated mean intensities, i.e., no polarization. These ratios are given in order to illustrate the large effect that polarization has on the measured line ratios. For example, at 6.86 keV line z has almost no polarization, line w is polarized about 58%, line x is polarized about -52% , and line y is polarized about -20% (Inal and Dubau¹⁵).

The 9.94-keV results involve more than one atomic process. The most important process is IEC. We have calculated the IEC contribution explicitly for $n = 3$ through $n = 5$ for s , p , and d levels using the cross sections calculated by Sampson, Parks, and Clark⁹ and the cascade matrix calculated by Pradhan.¹⁴ We have extrapolated these results to include all s , p , and d levels through $n = 10$. We find that the RR of Fe^{25+} contributes less than 3% of the total due to all other processes, and therefore RR is neglected. The calculated line ratios for the 9.94-keV case are also given in Table II. Again, calculations in parentheses refer to unpolarized lines.

Theory indicates that the contribution of IEC at 9.94 keV to the total rates is about 7%, 27%, 17%, and 82% for lines w , x , y , and z , respectively (see Fig. 1). Since the IEC component may be polarized differently than the components due to direct excitation, we have only estimated the effect of polarization on the y/w and x/w ratios in the 9.94-keV case. Two estimates are given assuming (a) the IEC component has the same polarization as

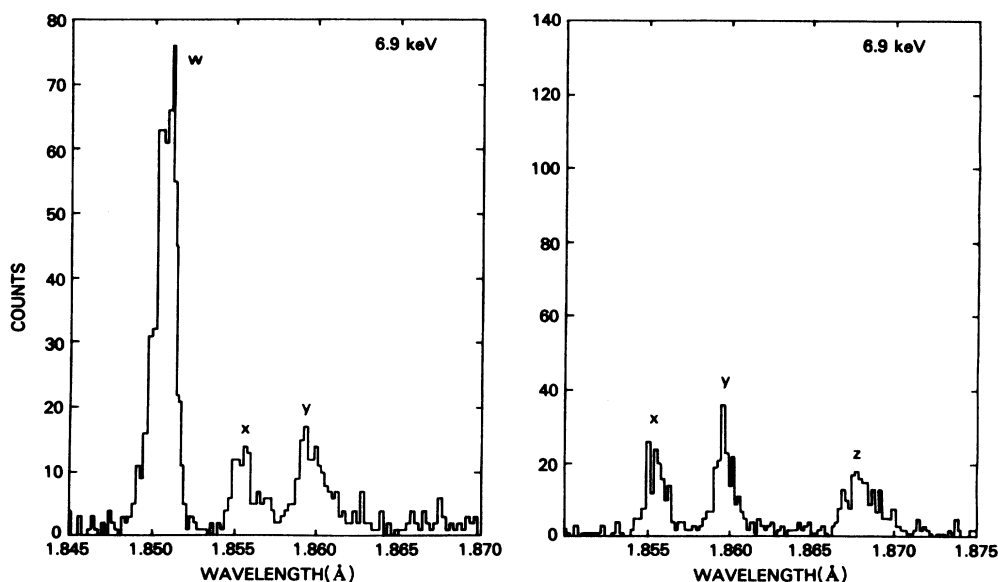


FIG. 2. Spectra of w , x , y , and z obtained at 6.86 keV.

TABLE II. Theoretical intensity ratios computed from direct IE cross sections and cascades at 6.86 and 9.94 keV.

Electron-beam energy (keV)	x/w	y/w	z/w
6.86 Bely-Dubau <i>et al.</i> ^b Inal and Dubau ^c	0.19 (0.39) ^a	0.20 (0.34)	0.23 (0.34)
6.86 Jones ^d Inal and Dubau ^c	0.19 (0.40)	0.20 (0.35)	0.23 (0.34)
9.94 Sampson, Parks, and Clark ^e Bely-Dubau <i>et al.</i> ^b Pradhan ^h Inal and Dubau ^c	0.088 ^e , 0.075 ^f (0.16)	0.13 ^e , 0.13 ^f (0.18)	(0.32)

^a Line ratios in parentheses refer to unpolarized (isotropic) radiation. The other line ratios include the theoretical angular distribution and the effects of the Ge(220) crystal on line intensities due to polarization. They are directly comparable to the measured ratios in Table I.

^b Reference 10.

^c Reference 15.

^d Reference 13.

^e Cascade-produced radiation is assumed to be unpolarized.

^f Cascade-produced radiation polarization is assumed to be the same as the polarization of the direct excitation radiation.

^g Reference 9.

^h Reference 14.

the direct component, and (b) the IEC component is unpolarized.

A comparison of Tables I and II shows good agreement between experiment and theory for x/w and z/w line ratios at 6.86 keV. The measured y/w ratio is slightly larger than theory.

At 9.94 keV it is only possible at present to compare the measured x/w and y/w ratios with theory, since line z is produced more by cascade than direct excitation, and the cascade polarization is unknown. We find measured ratios that are about 1.5 times larger than theory for the x/w and y/w ratios. A comparison of the 6.86- and 9.94-keV results suggests that the theoretical ratios are more accurate at energies close to threshold than for higher energies.

However, we should note that recent ongoing work at LLNL with the EBIT suggests that additional recombination mechanisms (not yet quantified) may exist other

than radiative recombination from the beam electrons considered above. Recombination mechanisms would enhance triplet to singlet ratios. Therefore the above conclusion concerning the comparison with theory and experiment at 9.94 keV should be regarded with caution.

The work at the Naval Research Laboratory was supported by the Strategic Defense Initiative Organization, and partly by a NASA grant from the Solar Physics Branch of the Space Physics Division. The work at LLNL was performed under the auspices of the U.S. Department of Energy under Contract No. W-7405-ENG-48. We thank Dr. Eric M. Gullikson for carrying out the calculations of crystal reflectivities used to deduce the effect of the Ge(220) crystal on line ratios. We thank Dr. J. Dubau for helpful comments on the polarization theory.

¹A. H. Gabriel, *Mon. Not. R. Astr. Soc.* **160**, 99 (1972).

²G. A. Doschek and K. Tanaka, *Astrophys. J.* **323**, 799 (1987).

³U. Feldman, G. A. Doschek, and J. F. Seely, *J. Opt. Soc. Am. B* **5**, 2237 (1988).

⁴M. Bitter *et al.*, *Phys. Rev. Lett.* **43**, 129 (1979).

⁵F. Bely-Dubau *et al.*, *Phys. Rev. A* **26**, 3459 (1982).

⁶TFR Group, J. Dubau, and M. Loulergue, *J. Phys. B* **15**, 1007 (1981).

⁷R. Giannella, *J. Phys. Colloq. Suppl.* **49** (3), C1-283 (1988).

⁸J. R. Lemen, K. J. H. Phillips, R. D. Cowan, J. Hata, and I. P. Grant, *Astron. Astrophys.* **135**, 313 (1984).

⁹D. H. Sampson, A. D. Parks, and R. E. H. Clark, *Phys. Rev. A* **17**, 1619 (1978).

¹⁰F. Bely-Dubau, J. Dubau, P. Faucher, and A. H. Gabriel, *Mon. Not. R. Astr. Soc.* **198**, 239 (1982).

¹¹A. K. Pradhan, *Astrophys. J. Suppl.* **59**, 183 (1985).

¹²P. Faucher and J. Dubau, *Phys. Rev. A* **31**, 3672 (1985).

¹³M. Jones, *Mon. Not. R. Astr. Soc.* **169**, 211 (1974).

¹⁴A. K. Pradhan, *Astrophys. J.* **288**, 824 (1985).

¹⁵M. K. Inal and J. Dubau, *J. Phys. B* **20**, 4221 (1987).

¹⁶M. A. Levine, R. E. Marrs, J. R. Henderson, D. A. Knapp, and M. B. Schneider, *Phys. Scr. T* **22**, 157 (1988).

¹⁷R. E. Marrs, M. A. Levine, D. A. Knapp, and J. R. Henderson, *Phys. Rev. Lett.* **60**, 1715 (1988).

¹⁸A. Henins, *Rev. Sci. Instrum.* **58**, 1173 (1987).

¹⁹B. P. Duval, J. Barth, R. D. Deslattes, A. Henins, and G. G. Luther, *Nucl. Instrum. Methods* **222**, 274 (1984).

²⁰J. F. Seely, U. Feldman, and U. I. Safronova, *Astrophys. J.* **304**, 838 (1986).

²¹A. Henins (private communication).

²²E. M. Gullikson (private communication).